

## Multi-Coil Shimming of the Mouse Brain

C. Juchem<sup>1</sup>, P. B. Brown<sup>1</sup>, T. W. Nixon<sup>1</sup>, S. McIntyre<sup>1</sup>, D. L. Rothman<sup>1</sup>, and R. A. de Graaf<sup>1</sup>  
<sup>1</sup>MR Research Center, Yale University, New Haven, CT, United States

**INTRODUCTION:** MR imaging and spectroscopy allow the non-invasive measurement of brain function and physiology, but excellent magnetic field homogeneity is required for meaningful results. The homogenization of the mouse brain (i.e. shimming) is a difficult task due to complex susceptibility-induced field distortions. To date, the achievement of satisfactory whole brain shimming in the mouse remains a major challenge.

After the introduction of the multi-coil (MC) approach for magnetic field modeling [1] and its first experimental application for shimming [2], here the homogenization of the mouse brain with static and dynamically updated MC fields is presented and compared to conventional shimming that is based on spherical harmonic (SH) basis functions.

**METHODS:** The MC fields for the homogenization of the mouse brain were synthesized from magnetic field shapes of 48 individual, circular coils (30 turns, diameter 13 mm, Fig. 1). The coils were made of copper wire and mounted in 6 rings of 8 coils each on the inside of an acrylic former with an inner diameter of 35 mm. A specific shim field was generated by driving the coils with a set of 48 optimized coil currents as described in [1]. Custom-built amplifier electronics allowed the adjustment of the currents in as little as 10  $\mu$ s throughout the dynamic range of  $\pm 1$  A [3]. A custom-built Bolinger RF antenna was placed inside the multi-coil setup to surround the mouse head and was used for RF transmission and signal reception. For comparison, conventional shimming based on the first and second order SH field terms was applied with the scanners' shim coil system. Magnetic field maps were calculated from seven single-echo gradient-echo images (field-of-view 15 x 15 x 22 mm<sup>3</sup>, matrix 75 x 75 x 44, echo time delays 0 / 0.1 / 0.2 / 0.5 / 1.0 / 2.0 / 3.0 ms). Three different methods for the homogenization of the mouse brain were compared: 1) Global, static SH shimming, 2) global, static MC shimming and 3) dynamic MC shimming for which the fields were optimized and updated over a stack of coronal slices. The field homogeneity in 7 mice at 9.4 Tesla after shimming was assessed by the standard deviation of the field distribution over the whole brain (Fig. 2) and via the impact of the shimming on the quality of gradient-echo images at settings typically used for functional MRI.

All magnetic field measurements, data analysis and hardware handling were done with custom-made software and methods.

**RESULTS:** Static MC shim fields allowed the reduction of the standard deviation of the observed Larmor frequencies by 31% (Fig. 2C) compared to SH shimming (Fig. 2B). MC shimming with the dynamic, slice-specific application of the shim fields led to largely flat field distributions over the mouse brain (Fig. 2D) with a 66% average narrowing of the fields' standard deviation compared to SH shimming. For gradient-echo imaging at 15 ms echo time, static and dynamic MC shimming consistently minimized the shim-related signal voids in the brain periphery and overall signal gains of 40-50% were achieved with the dynamic approach compared to SH shimming (Fig. 3).

**DISCUSSION:** The magnetic fields generated by a set of generic circular coils were shown to be capable of compensating the field distortions encountered in the mouse brain at 9.4 Tesla. The novel MC concept enabled the flexible and accurate generation of complex magnetic field shapes that allowed significantly improved magnetic field homogenization of the mouse brain compared to conventional SH shimming. The MC shimming technique paves the way for MR applications of the mouse brain as a whole or parts thereof for which excellent magnetic field homogeneity is a prerequisite.

This research was supported by NIH grants R21/R33-CA118503, R01-EB000473 and P30-NS052519

[1] J Magn Reson 2010, 204:281-289; [2] Proc. ISMRM (2010), 1535; [3] Proc. ISMRM (2010), 1532.

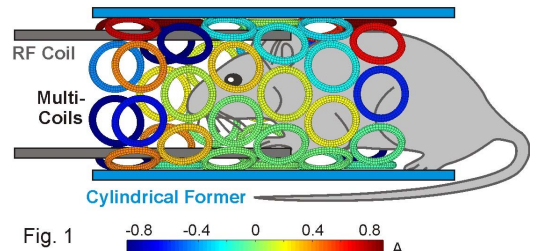


Fig. 1 -0.8 -0.4 0 0.4 0.8 A

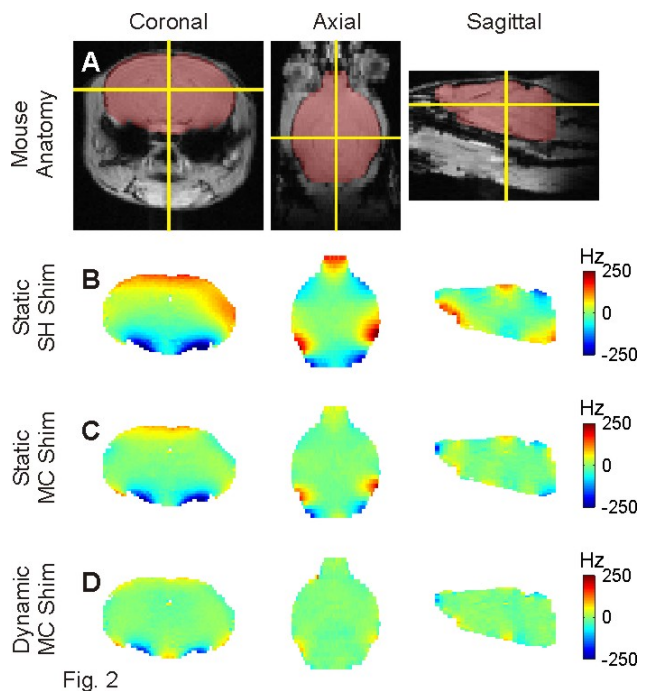


Fig. 2

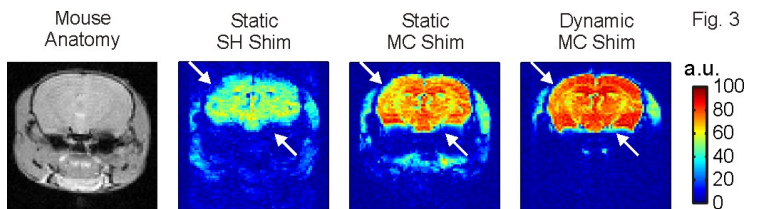


Fig. 3